Astrophys. Space Sci. Trans., 7, 131–136, 2011
www.astrophys-space-sci-trans.net/7/131/2011/
doi:10.5194/astra-7-131-2011

ASTRA
Astrophysics and Space Sciences Transactions

Cosmic ray physics with the ARGO-YBJ experiment

A. Surdo (on behalf of the ARGO-YBJ Collaboration)

INFN – Sezione di Lecce, via Arnesano, 73100 Lecce, Italy

Received: 12 November 2010 – Accepted: 19 January 2011 – Published: 19 April 2011

Abstract. The main scientific goals of the ARGO-YBJ experiment are γ-ray astronomy with a few hundreds GeV energy threshold and cosmic ray physics below and around the knee of the primary energy spectrum ($10^{12} - 10^{16}$ eV), where the transition from direct to indirect measurement techniques takes place. The ARGO-YBJ experiment, located at the Cosmic Ray Observatory of Yangbajing (Tibet, P.R. of China, 4 300 m a.s.l.), is an unconventional Extensive Air Shower array of about $6,700\,\mathrm{m}^2$ of active area, the only one exploiting the full-coverage technique at very high altitude currently in operation. The detector space-time granularity, performance and location offer a unique chance to make a detailed study of the structure of cosmic ray showers, in particular of the hadronic component. In this work we will focus on the main experimental results concerning cosmic ray and hadronic interaction physics: primary cosmic ray energy spectrum, antiproton over proton ratio, anisotropy in the cosmic ray flux and proton-air cross-section. Moreover, the possible data analysis improvements based on the use of all detailed information on the shower front (curvature, time width, rise time, ..), as well as the extension of the investigable energy range, allowed by the analog RPC readout, will be pointed out.

1 Introduction

As a result of the collaboration between INFN (Italy) and Chinese Academy of Sciences, the ARGO-YBJ (Astrophysical Radiation with Ground-based Observatory at YangBaJing) experiment (see Bacci et al., 2002, and references therein) is operating at the YangBaJing Cosmic Ray Laboratory (Tibet, P.R. China, 4 300 m a.s.l.). It is the only air shower array in the world exploiting the full-coverage technique at very high altitude presently in data taking. Location and detector features make ARGO-YBJ capable of investigating a wide range of fundamental issues in Cosmic Ray and Astroparticle Physics at relatively low energy threshold:
- very high energy γ-ray astronomy, with an energy threshold of a few hundreds GeV;
- search for emission of gamma ray bursts in the full GeV – TeV energy range;
- study of cosmic rays (spectrum, composition, $\overline{p}/p$ ratio measurement, shower space-time structure, ...) starting at TeV energies;
- Sun and heliosphere physics above $E_{th} \sim 1$ GeV.

In following sections, after a brief description of the detector and its performance, the main results achieved on several items of cosmic ray physics will be presented and discussed.

2 The detector

The ARGO-YBJ detector consists of a single layer of Resistive Plate Chambers (RPCs) operating in streamer mode (Aielli et al., 2006). The full-coverage central detector, having an extension of about $5800\,\mathrm{m}^2$ ($\sim 92\%$ of active area), is surrounded by a partially instrumented ($\sim 40\%$) guard ring mainly to improve the discrimination capability of external events. The apparatus has a modular structure, the basic element being a *cluster* (the DAQ basic unit), of dimensions $5.7 \times 7.6\,\mathrm{m}^2$, constituted by 12 RPCs ($1.25 \times 2.80\,\mathrm{m}^2$ each). Each RPC is read by 80 strips ($6.75 \times 61.8\,\mathrm{cm}^2$ each) representing the spatial pixels, logically organized in 10 pads of $55.6 \times 61.8\,\mathrm{cm}^2$, which are individually acquired and constitute the detector time pixel. The full detector is made by 153 clusters for a total active surface of $\sim 6,700\,\mathrm{m}^2$. The RPC charge read-out has also been implemented by instrumenting every chamber with two large size pads ($125 \times 140\,\mathrm{cm}^2$ each), in order to extend the dynamic range up to $\sim$ PeV energies (Iacovacci et al., 2009).

Correspondence to: A. Surdo
(antonio.surdo@le.infn.it)

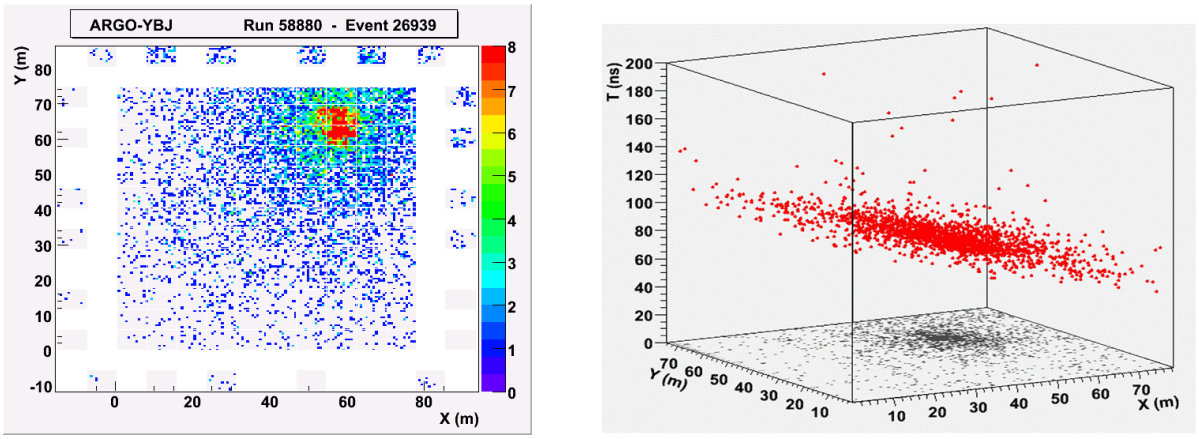

Fig. 1. The pad image of a shower detected by ARGO-YBJ. The colour scale represents the strip multiplicity of each fired pad (left). The space-time view of the shower front is also shown (right).

The detector operates simultaneously in two different and independently working modes: shower and scaler. In shower mode, for each event the position and timing of every detected particle is recorded, allowing the reconstruction of the core location, the lateral distribution and the arrival direction of the shower. In scaler mode the total counts on each cluster are measured every 0.5 s, with limited information on both the space distribution and arrival direction of the detected particles, in order to lower the energy threshold down to ~ 1 GeV (Aielli et al., 2008, 2009a,b).

Since November 2007 the detector (guard ring included) is in stable data taking with a multiplicity trigger $N_{pad} \geq 20$ and a duty cycle $\geq 85\%$: the trigger rate is about 3.6 kHz.

3 Moon shadow and detector performance

The detector space granularity and time resolution (at level of ~ 1 *ns*) allow the three-dimensional reconstruction of the shower front with unprecedented details (Fig. 1). The performance and the operation stability of the detector are continuously monitored by observing the Moon shadow, i.e. the deficit of cosmic rays (CR) caused by the Moon absorption. Indeed, the size of the deficit allows the measurement of the angular resolution while its position allows the evaluation of the absolute pointing accuracy of the detector. In addition, positively charged particles are deflected towards East due to the geomagnetic field by an angle depending on energy: $\Delta\theta \sim 1.6^\circ Z/E$ TeV. Therefore, the observation of the displacement of the Moon provides a direct calibration of the relation between shower size and primary energy.

Figure 2 shows the significance map of the Moon region with the detected deficit. With all data from July 2006 to December 2009 (about 3200 h on-source in total) we observed the CR Moon shadowing effect with a significance of about 55 standard deviations (s.d.). The amount and shape of the CR deficit is the convolution of the point spread function of the detector and the widespread Moon disc. The measured angular resolution is better than 0.5° for showers with energies $E > 5$ TeV and the overall absolute pointing accuracy is at a level of $\sim$0.1°. The accuracy of the energy scale determination is estimated to be less than 18% in the energy range $1-30$ TeV/Z.

The Moon shadow observation has also been used for a measurement of the CR $\overline{p}/p$ ratio, as discussed in Sect. 6.

4 Observation of the Sun shadow

In a similar way, the Sun also causes a shadowing effect on cosmic rays coming from its direction, clearly shown in Fig. 3 as a result of the analysis of ARGO-YBJ data collected since July 2006 up to December 2009 (Aielli et al., 2011).

In this case, an important role is also played by the magnetic field along the path from the Sun to the Earth, which deflects the primary charged particles from straight trajectories, producing a shift of the shadow from the true Sun position. Thus, in principle, the study of the Sun shadow and its variations could permit to measure and monitor in time the Interplanetary Magnetic Field (IMF). Nevertheless, the deficit significance and position are strongly correlated to the solar activity, so that IMF is better studied in quiet phases of the Sun. The ARGO-YBJ observation reported in Fig. 3 refers just in such a particularly good time window when solar activity stays at its minimum since 2006. In particular, the detected North-South displacement of the shadow from the Sun position is mostly related to the effect of IMF action.

5 Light-component Cosmic Ray spectrum

A first measurement of the differential energy spectrum of the primary CR light component (p+He) has been performed by ARGO-YBJ applying a Bayesian unfolding approach to

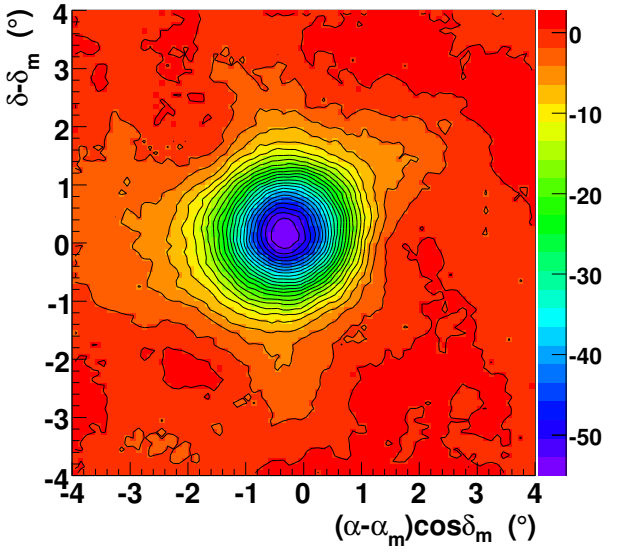

Fig. 2. Moon shadow significance map for events with $N_{pad} \geq 100$ fired pads. The colour scale gives the significance.

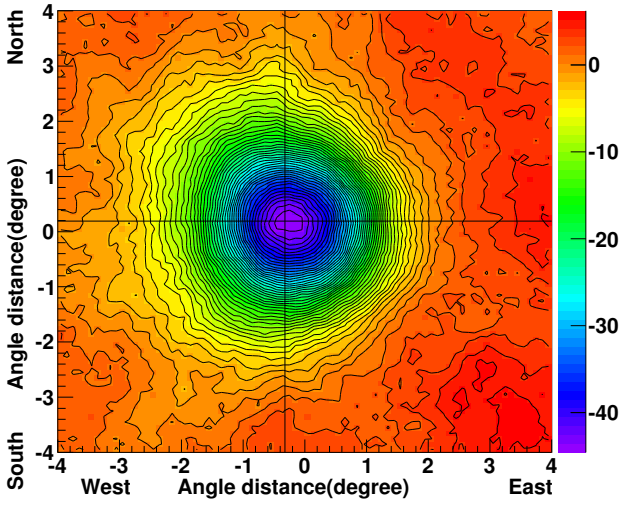

Fig. 3. Sun shadow significance map for events with $N_{pad} \geq 100$ fired pads. The colour scale gives the significance.

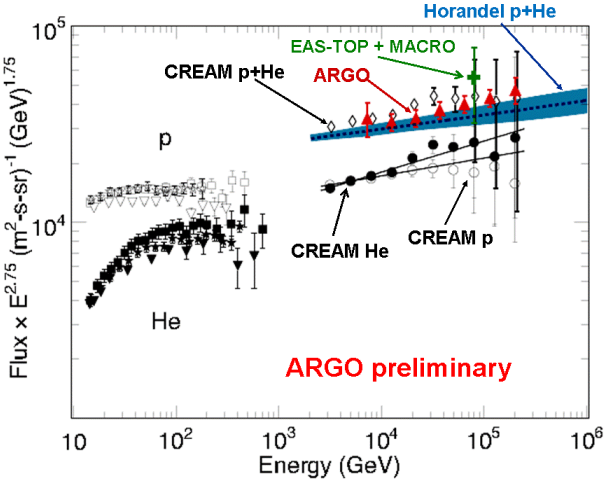

Fig. 4. Light-component (p+He) differential spectrum of primary CRs measured by ARGO-YBJ and compared with other experimental results.

the strip multiplicity spectrum. The results are briefly outlined here, more details can be found in We selected showers with zenith angle $\theta < 30°$ and with reconstructed core position inside a fiducial area $50 \times 50\,\mathrm{m}^2$ large by applying a selection criterion based on the fired strip density. According to Monte Carlo (MC) simulations, in the investigated energy range, the contamination of nuclei heavier than Helium (mainly CNO and Iron) is found to be negligible, not exceeding a few percents (thanks to the event selection cuts). On the other side, the present analysis does not allow the determination of the individual proton and Helium contribution to the measured flux.

In Fig. 4, the result by ARGO-YBJ (filled triangles) in the energy region $5 - 250\,\mathrm{TeV}$ is compared with other experiments. We note that the ARGO-YBJ measures agree remarkably well with the values obtained by adding up the proton and helium fluxes measured by the CREAM experiment in the same energy range, concerning both the total intensities and the spectrum (Ahn et al., 2010). The value of the spectral index of the power-law fit representing the ARGO-YBJ data is -2.61 ± 0.04, which should be compared to $\gamma_p = -2.66 \pm 0.02$ and $\gamma_{He} = -2.58 \pm 0.02$ obtained by the CREAM experiment.

It is worth to stress that for the first time direct and ground-based measurements overlap for a wide energy range thus making possible the cross-calibration of the different experimental techniques.

6 Measurement of the $\overline{p}/p$ ratio

The study of the Moon shadow permits to measure the $\overline{p}/p$ ratio in CR flux: if protons are deflected towards East, antiprotons are deflected towards West. If the energy is low enough and the angular resolution small we can distinguish, in principle, between two shadows, one shifted towards West due to the protons and the other shifted towards East due to the antiprotons. If no event deficit is observed on the anti-matter side an upper limit on the antiproton content can be calculated. In the ARGO-YBJ experiment, the angular resolution is small enough for events with at least ~ 40 fired pads, thus allowing such a measurement at few TeV energy range (Di Sciascio et al., 2009).

As showed in Sect. 2, with all data up to December 2009 we detected the Moon shadow on CRs with a significance of about 55 s.d. (3200 h on-source). We selected 2 multiplicity bins, 40<N<100 and N>100. In the first interval the statistical significance of the Moon shadow is 34 s.d., the measured

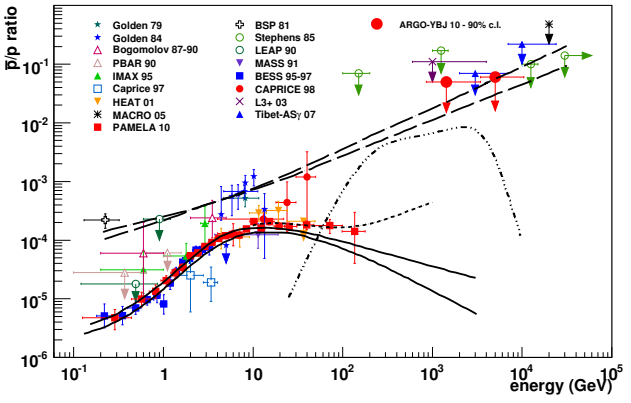

Fig. 5. The measure of the $\overline{p}/p$ ratio obtained with the ARGO-YBJ experiment compared with all available measurements. The solid curves refer to a direct production model. The dashed lines refer to a model of primary $\bar{p}$ production by antigalaxies (Stecker, 1985). The rigidity-dependent confinement of cosmic rays in the Galaxy is assumed to be $\propto R^{-\delta}$, and the two dashed curves correspond to the cases of δ = 0.6, 0.7. The dotted line refers to the contribution from a heavy Dark Matter particle annihilation (Cirelli, 2009).

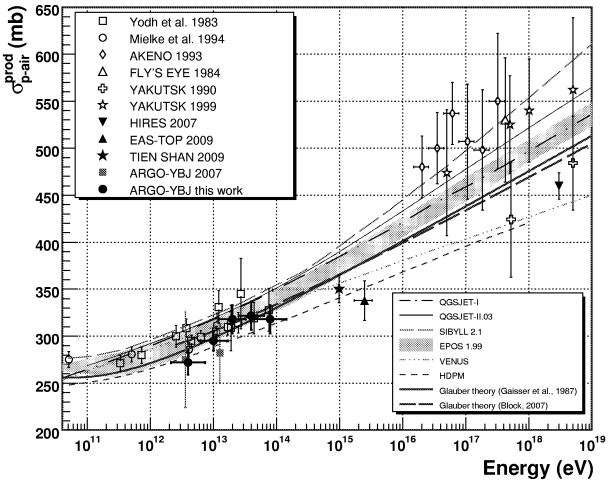

Fig. 6. Proton-air production cross section measured by ARGO-YBJ and by other CR experiments. The predictions of two different calculations based on Glauber theory are also shown.

angular resolution is ∼1° and the median energy is 1.4 TeV. For N>100 the significance is 55 s.d., the angular resolution is ∼0.6° and the median energy is 5 TeV. With all the data up to December 2009 we set two upper limits to the $\overline{p}/p$ ratio at the 90% confidence level: 5% at 1.4 TeV and 6% at 5 TeV. The upper limits calculated with ARGO-YBJ are compared in Fig. 5 with all the available $\overline{p}/p$ measurements and with some theoretical models for antiproton production.

7 Measurement of the total p-p cross section

To make this measurement, the ARGO-YBJ data analysis is based on the shower flux attenuation for different zenith angles, i.e. atmospheric depths, and exploits the detector accuracy in reconstructing the shower properties. For fixed primary energy and shower age, such an attenuation is expressed by the absorption length, Λ, connected to the primary (mainly protons) interaction length in the atmosphere by the relation: $\Lambda = k \cdot \lambda_{CR}$, where k depends on the shower development in the atmosphere, on its fluctuations and on the detector response. The actual value of k must be evaluated by MC simulations, and it might in principle depend on the features of the adopted hadronic interaction model, even if several studies showed that the dependence is small. In this analysis, a full simulation chain was used, with the production of a suitable sample of proton and He primary showers by means of the CORSIKA code (with three different hadronic interaction models) and the detector response simulation based on the GEANT package (**?**), including the effects of time resolution, trigger logic, electronics noise, etc. For primary protons, the interaction length is related to the p-air interaction cross-section by: $\lambda_p(g/cm^2) \simeq 2.41 \cdot 10^4/\sigma_{p-air}(mb)$. Given a primary energy interval, the frequency of showers as a function of the zenith angle θ, for a fixed distance X_{dm} between the detector and the shower maximum, is directly related to the distribution of the depth of the shower maximum itself, $P(X_{max})$, with $X_{max} = h_0 sec\theta - X_{dm}$, where h_0 is the observation vertical depth (= 606 g/cm^2 at the Yangbajing altitude). It can be shown that for enough large X_{max} values, $P(X_{max})$ tends to have a simple exponential falling behaviour, so as the shower frequency distribution, as a function of the zenith angle. In fact, the exponential tail of that distribution can be accessed by selecting the showers with the maximum development not far from the detection level (i.e. by minimizing X_{dm}) and, obviously, exploring a zenith angle region as wide as possible. With these objectives, the ARGO-YBJ detector location (i.e. small atmospheric depth) and features (full-coverage, angular resolution, fine granularity, etc.), which ensure the capability of reconstructing very carefully the detected showers, have been exploited (see Surdo et al., 2008; Aielli et al., 2009c, for the analysis details).

The measured p-air production cross section as a function of the primary proton energy is reported in Fig. 6. The results found by other experiments an the predictions of several hadronic interaction models are also shown. The systematics arising from several sources have been taken into account and evaluated on the basis of the MC simulation. In particular, the contribution coming from heavy nuclei contained in the primary cosmic ray flux have been estimated by adding a proper He fraction to the proton primary flux in the MC (the contribution of nuclei heavier than α particles is negligible).

Finally, Glauber theory has been used to infer the total proton-proton cross section σ_{p-p} from the measured

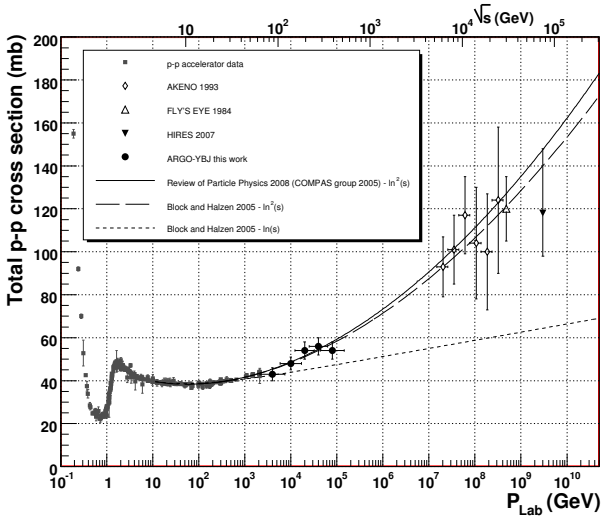

Fig. 7. Total p-p cross section obtained by ARGO-YBJ starting from σ_{p-air} together with the same quantity measured at accelerators and by other CR experiments (Amsler et al., 2008).

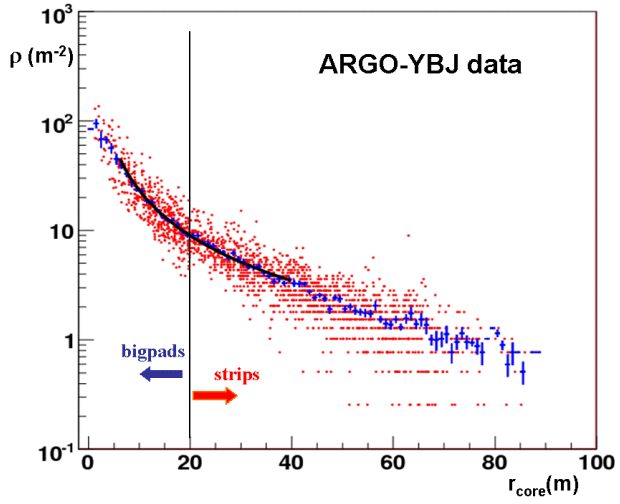

Fig. 8. Lateral density function of showers detected by ARGO-YBJ, as reconstructed from RPC charge information up to ∼20 m from the core, while the strip information are used for larger distances.

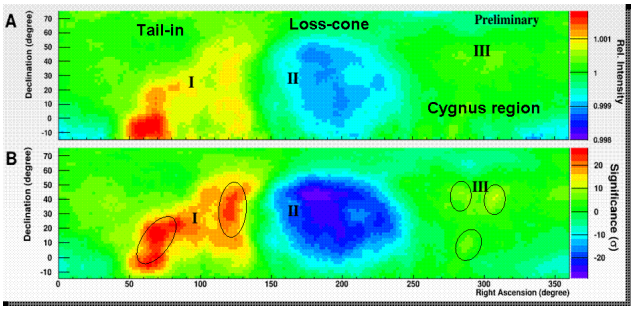

Fig. 9. Large scale CR anisotropy observed by ARGO-YBJ at energies ∼2 TeV. In the upper plot the colour scale gives the relative CR intensity, in the lower plot the statistical significance in standard deviations.

proton-air production cross section σ_{p-air} (see for instance Gaisser, 1987; **?**, and references therein). The results are shown in Fig. 7 for the five considered energy values. Also shown in the figure are the measurements made at accelerators and by other CR experiments starting from σ_{p-air}. As can be seen, the ARGO-YBJ data lie in an energy region scarcely explored by accelerator experiments and permit of better investigating the behaviour of the p-p total cross section where it starts to significantly increase with energy. In particular, our result favours the asymptotic $ln^2(s)$ increase of total hadronic cross sections as obtained in (Block, 2005) from a global analysis of accelerator data.

Concerning the possible development of this analysis, the use of the analog RPC charge readout will allow to extend the study to collisions with center-of-mass energies up to the ∼TeV region. On the other hand, it will provide a much more accurate shower size and lateral density profile determination, thus giving a more reliable reconstruction of physical quantities (Fig. 8). Moreover, further improvements are expected from the use of several detailed information on the shower front (curvature, rise time, time width, etc.), that ARGO-YBJ is able to record with very high precision. This could give a better constraint on the longitudinal shower profile and $X_{\max}$ depth, which, as already stated, is a crucial point for minimizing shower development fluctuations (thus reducing the sistematic uncertainty).

8 Large and Medium scale anisotropies

Galactic Cosmic Rays at TeV energies are expected to appear highly isotropic, since during their propagation from the sources to the Earth they undergo complex processes, such as the deflection by the large scale Galactic magnetic field and the interaction with background photons and interstellar medium. Thus the study of the galactic CR anisotropy is a useful tool in probing the magnetic field structure in our interstellar neighbourhood as well as the source distribution.

Several experiments have reported two large-scale anisotropic structures, the so-called 'tail-in' and 'loss-cone' regions. With two years of data, ARGO-YBJ carried out a two-dim. (2D) measurement to investigate the detailed structural information of the large scale CR anisotropy beyond the simple Right Ascension (R.A.) profiles. The two anisotropic regions, correlated to an enhancement or deficit of CRs, are clearly visible with a significance of about 20 s.d. (Fig. 9). A new excess component with a ∼0.1% increase of the CR intensity in the Cygnus region is observed with a significance of about 10 s.d.. To quantify the scale of the anisotropy we fitted the 1D R.A. projection of the 2D map with the first two harmonics for three different energies. The preliminary results (E = 0.7 TeV, A_1=(3.6±0.1)·10^{-4}, ϕ_1=63.4°±0.9°; E =

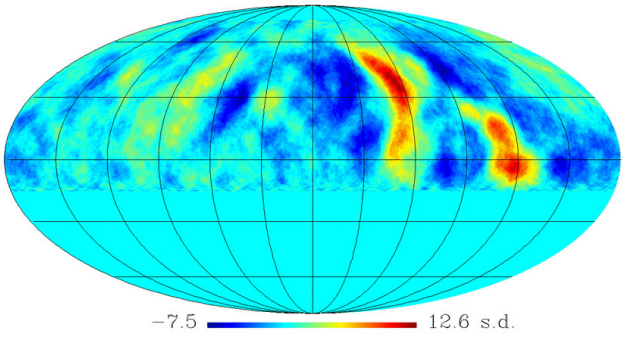

Fig. 10. Medium scale anisotropy of CRs at energies ~ 2 TeV. The colour scale gives the statistical significance in standard deviations.

1.5 TeV, $A_1=(6.8\pm0.1)\cdot10^{-4}$, $\phi_1=41.0°\pm0.7°$; E = 3.9 TeV, $A_1=(9.0\pm0.1)\cdot10^{-4}$, $\phi_1=35.3°\pm0.6°$) are in good agreement with other experiments (Guillian et al., 2007).

Using different analysis methods, ARGO-YBJ is able to observe anisotropies in all scale, including the intermediate one. Figure 10 shows the sky map for events with $N_{pad} \geq 40$ fired pads and zenith angle $\theta < 40°$ (corresponding to a proton median energy ~ 2 TeV), obtained with a 5° smoothing radius. The analysis has been performed in order to be insensitive to the CR large-scale anisotropy which is roughly one order of magnitude greater. The map clearly shows two large hot spots in the region of the Galactic anticenter. The two excesses (>10 s.d., corresponding to a flux increase of $\sim 0.1\%$), observed by ARGO-YBJ around the positions $\alpha \sim 120°$, $\delta \sim 40°$ and $\alpha \sim 60°$, $\delta \sim -5°$, are the same visible in the already shown tail-in region.

The origin of this anisotropy is puzzling. In fact, these regions have been interpreted as excesses of hadronic CRs, but TeV CRs are expected to be randomized by the magnetic fields. Understanding these anisotropies should be a high priority as they are probably due to a nearby source of CRs.

9 Conclusions

The ARGO-YBJ experiment is in stable data taking since November 2007 with a duty cycle $> 85\%$ and with very good performance. We observed the CR Moon and Sun shadows with a significance of 55 s.d. and 45 s.d., respectively. The detector performance is continuously monitored with the Moon shadow technique. The angular resolution has been stable at a level better than 10% over the last 2 years.

Several interesting results are available in particular in CR physics. The light-component (p+He) spectrum of primary CRs has been measured in the range $5-250$ TeV. The results are in good agreement with the CREAM balloon data. For the first time direct and ground-based measurements overlap for a wide energy range thus making possible the cross-calibration of the different experimental techniques. A measurement of the $\overline{p}/p$ ratio at few-TeV energies has been performed setting two upper limits at the 90% confidence level: 5% at 1.4 TeV and 6% at 5 TeV. In the few-TeV range these results are the lowest available, useful to constrain models for antiproton production in antimatter domains. The p-air production cross section has been measured in the range $1-100$ TeV and the corresponding $p-p$ total cross-section inferred. A medium-scale anisotropy has been observed with a significance greater than 10 s.d. at proton median energy of about 2 TeV. With 2 years of data we carried out a 2D measurement of the CR large-scale anisotropy to investigate detailed structural information beyond the simple Right Ascension profiles, finding a good agreement with other experiments.

Edited by: T. Suomijarvi
Reviewed by: two anonymous referees

References

Aielli, G. et al. (ARGO-YBJ Coll.): Layout and performance of RPCs used in ARGO-YBJ, NIM, A 562, 92–96, 2006.
Aielli, G. et al. (ARGO-YBJ Coll.): Scaler mode technique for the ARGO-YBJ detector, Astropart. Phys., 30, 85–95, 2008.
Aielli, G. et al. (ARGO-YBJ Coll.): Temperature effect on RPC performance in ARGO-YBJ, NIM, A 608, 246–250, 2009a.
Aielli, G. et al. (ARGO-YBJ Coll.): ARGO-YBJ constraints on VHE emission from GRBs, Astropart. Phys., 32, 47–52, 2009b.
Aielli, G. et al. (ARGO-YBJ Coll.): Proton-air cross section measurement with ARGO-YBJ, Phys. Rev., D 80, 092004-14, 2009c.
Aielli, G. et al. (ARGO-YBJ Coll.): Mean interplanetary magnetic field measurement in ARGO-YBJ, Astrophys. J., doi:10.1088/0004-637X/729/2/113, 2011.
Amsler, C. et al. (Particle Data Group): The review of particle physics, Phys. Lett., B 667, 1–1340, 2008.
Bacci, C. et al. (ARGO-YBJ Coll.): Results from the ARGO-YBJ test experiment, Astropart. Phys., 17, 151–165, 2002.
Block, M. M. and Halzen, F.: New evidence for the saturation of the Froissart bound, Phys. Rev., D 72, 036006–10, 2005.
Cirelli, M. and Strumia, A.: Minimal dark matter: model and results, New J.- Phys., 11, 105005–31, 2009.
Di Sciascio, G. et al. (ARGO-YBJ): Measurement of anti-p/p ratio with ARGO-YBJ, Proc. XXXI ICRC, 431–434, 2009.
Gaisser, T. K., Sukhatme, U. P., and Yodh, G. B.: Hadron cross sections at UHEs and unitarity bounds on diffraction, Phys. Rev., D 36, 1350–1357, 1987.
Guillian, G. Hosaka, J., Ishihara, K., et al.: Observation of the anisotropy of 10 TeV primary CR nuclei flux with SK-I, Phys. Rev., D 75, 062003–17, 2007.
Iacovacci, M. et al. (ARGO-YBJ): The charge readout system of the RPCs in ARGO-YBJ, Proc. XXXI ICRC, 1388, 2009.
Mari, S. M. et al. (ARGO-YBJ): The all-particle spectrum by means of a Bayesian unfolding technique with the ARGO-YBJ data, Proc. XXXI ICRC, 407, 2009.
Stecker, F. W. and Wolfendale, A. W.: Observation of antimatter in our Galaxy, Proc. XIX ICRC 2, 354, 1985.
Surdo, A. (ARGO-YBJ): Measurement of p-air inelastic cross section in ARGO-YBJ, Proc. XXI ECRS, Kosice (SK), 550, 2008.